



# Technical Note: Intermittent reduction of the stratospheric ozone over Northern Europe caused by a storm in Atlantic Ocean

Mikhail Sofiev<sup>1</sup>, Rostislav Kouznetsov<sup>1,2</sup>, Risto Hänninen<sup>1</sup>, Viktoria F. Sofieva<sup>1</sup>

<sup>1</sup>Finnish Meteorological Institute, Helsinki, 00560, Finland

5 <sup>2</sup>AM Obukhov Institute for Atmospheric Physics, Moscow, Russia

*Correspondence to:* Mikhail Sofiev (mikhail.sofiev@fmi.fi)

**Abstract.** A three-day episode of anomalously low ozone concentrations in the stratosphere over Northern Europe occurred on 3-5 November 2018. A reduction of the total ozone column down to ~200-210 Dobson Units was predicted by the global forecasts of System for Integrated modeLLing of Atmospheric coMposition (SILAM) driven by the weather forecast of  
10 Integrated Forecasting System (IFS) of European Centre for Medium-Range Weather Forecasting (ECMWF). The reduction down to 210-215 DU was subsequently observed by the satellite instruments, such as Ozone Monitoring Instrument (OMI) and Ozone Mapping Profile Suite (OMPS). The episode was caused by intrusion of the tropospheric air, which was initially  
15 uplifted by a storm in Northern Atlantic, south-east of Greenland. Subsequent transport towards the east and further uplift over Scandinavian ridge of this humid and low-ozone air brought it to ~25 km altitude causing ~30% reduction of the ozone layer thickness over Northern Europe. The low-ozone air was further transported eastwards and diluted over Siberia, so that  
the ozone concentrations restored a few days later. High accuracy of the episode prediction 5 days in advance by the IFS-SILAM modelling tandem illustrates the model capabilities of short-term forecasting of the stratospheric composition, including such rare events.

## 1 Introduction

20 The main stratosphere-troposphere exchange mechanism in extratropical regions is associated with synoptic-scale processes, in particular, extratropical cyclones (Jaeglé et al., 2017; Stohl, 2003). Attention is usually paid to intrusions of the stratospheric air into the troposphere along the descending dry-intrusion air streams of the cyclonic structure (Ebel et al., 1991; Jaeglé et al., 2017; Reutter et al., 2015; Stohl, 2001, 2003). These intrusions are estimated to be responsible for about  
25 450-500 Tg of annual ozone import in the troposphere, which is about 10% of the ozone chemical production in the troposphere (Edwards and Evans, 2017; Olsen et al., 2013; Roelofs and Lelieveld, 2000). The uplift of the tropospheric air occurs along the ascending warm conveyor belt (WCB) of the cyclonic structure (Stohl, 2001). The dry-intrusions – WCB mechanism is responsible for 40-60% of the intrusions in the middle latitudes over Atlantic Ocean (Reutter et al., 2015). It has been suggested that these intrusions are quite shallow, i.e. the majority of the plumes do not penetrate significantly beyond the UTLS (Upper-Troposphere-Lower-Stratosphere) interface. For the stratosphere-to-troposphere (STT) intrusions,



in particular, the fraction of streams reaching middle troposphere is suggested to be just 15% (Jaeglé et al., 2017). The bulk of works on the stratosphere-troposphere exchange concentrate on its role in the ozone budget of the troposphere.

In the above works, as well as in the earlier studies (see references in the reviews of Stohl, 2003 and Jaeglé et al., 2017), a dominant proposition is that the intrusions related to the troposphere-to-stratosphere transport (TST) do not reach high altitudes predominantly staying within the UTLS layer where their impact on the ozone concentrations is comparatively small. Exceptions are the moist deep-convective updraughts in the tropics reaching up to 50 hPa (20km altitude) and pollution injection up to 80-100hPa (17-19 km) by Asian monsoon (Orbe et al., 2015). The deep penetration of the tropospheric air into the stratosphere leads to the corresponding reduction of the ozone layer. However, outside the tropical regions and areas affected by the Asian monsoon the TST events are practically not considered.

10 The current short note analyses an unusual event that took place in the beginning of November 2018 and initially looked like a typical extratropical cyclone with sea-level pressure in the centre being just under 960 hPa. However, the WCB plume was eventually uplifted to 20-25 km and significantly affected the stratospheric ozone layer over northern Fennoscandia (60N-70N) two days later.

15 In the following section, we present the SILAM model, which forecasted the episode 5 days in advance, and outline the satellite information, which was used to confirm the event and to validate the forecasts retrospectively. The episode development is followed using the model simulations, which are evaluated against the satellite retrievals. Finally, we provide a short overview of similar historical events and estimate the significance of the current episode from the large-scale standpoint.

## 2 Forecasting model and observational data

### 20 2.1 SILAM model and input data

System for Integrated modeLLing of Atmospheric coMposition (SILAM, <http://silam.fmi.fi>, (Sofiev et al., 2015)) is an offline chemistry-transport model covering the troposphere and the stratosphere and providing the global and regional forecasts up to 5 days ahead for 113 species. The model chemistry transformation scheme consists of: (i) modified CBM4 mechanism (Gery et al., 1989) with updated chemistry rates, (ii) heterogeneous inorganic chemistry of (Sofiev, 2000) expanded with marine boundary layer nitrate formation, (iii) Volatility-Basis Set for the secondary organic aerosols, (iv) Polar Stratospheric Cloud (PSC) formation generally following (Carslaw et al., 1995) for supercooled ternary solutions of  $\text{HNO}_3 + \text{H}_2\text{SO}_4$  and the formulations of the FinROSE model (Damski et al., 2007) for nitric acid trihydrate (NAT) and ice aerosols, (v) gas-phase chemistry transformations in the stratosphere of FinROSE with an extended set of halogenated species and updated and extended set of photolysis reactions.

30 Input meteorological data for the SILAM forecast are taken from the Integrated Forecasting System (IFS) of European Centre for Medium-Range Weather Forecast (ECMWF, <http://www.ecmwf.int>, accessed 10.04.2019). The data are used in lon-lat projection with horizontal resolution of  $0.2^\circ \times 0.2^\circ \times 3$  hr and 135 vertical levels reaching up to ~4 Pa.



Emission data are compiled from several sources. The main anthropogenic emission dataset is MACCITY (Granier et al., 2011) with shipping excluded. It is complemented with the shipping emission inventory produced with the STEAM model (Jalkanen et al., 2009, 2016; Sofiev et al., 2018). Biomass burning emission and its injection profile are calculated in real-time by IS4FIRES (<http://is4fires.fmi.fi>, accessed 10.04.2019, (Sofiev et al., 2009, 2013)) for aerosols and taken from the  
5 GFAS dataset (Kaiser et al., 2009) for gases. Biogenic emission is taken from the MEGAN computations (Sindelarova et al., 2014). Supplementary datasets include RETRO-aircraft (Grewe, pers.comm.), GEIA NO<sub>x</sub> from lightning (Price et al., 1997) and GEIA reactive chlorine compounds (Lobert et al., 1999) and CFCs (Cunnold et al., 1994) emissions. The emission of sea salt, wind-blown dust and DMS are computed online by SILAM (Sofiev et al., 2011). Finally, the compensating emission of N<sub>2</sub>O was estimated from the global mass budget conservation requirement and is introduced as a homogeneous constant flux  
10 from the land areas, except for Antarctica.

The SILAM forecast is run daily, 5 days ahead, with the global horizontal resolution of 0.2°×0.2° and 29 vertical levels reaching up to 5.25 Pa (mid-point of the last layer). The model does not use data assimilation and the initial conditions are taken from the previous-day forecast. Hourly averaged 3D fields of concentrations and 2D fields of dry and wet deposition, as well as aerosol column optical thickness constitute the model output presented at the model Web site <http://silam.fmi.fi>  
15 (accessed 10.04.2019) in both graphical and numerical forms.

## 2.2 Satellite observations

Current study used three sets of the satellite data: from Ozone Monitoring Instrument OMI (<https://aura.gsfc.nasa.gov/omi.html>, accessed 10.04.2019, (Levelt et al., 2006, 2018)) and Ozone Mapping Profiler Suite (OMPS, <https://jointmission.gsfc.nasa.gov/omps.html>, accessed 10.04.2019, (Flynn et al., 2006)). Both satellites observe  
20 total ozone column over cloud-free areas and stratospheric ozone column above the clouds. Below, we present the Level 2 OMI total ozone column data with removed row-anomaly (the OMPS observations show very similar patterns). Vertical ozone profile evaluation was based on retrievals of Microwave Limb Sounder v 4.2 (MLS, <https://mls.jpl.nasa.gov/>, accessed 10.04.2019, (Waters et al., 2006)).

For the evaluation, full space- and time- collocation was applied at hourly level, i.e. we used only those grid cells of the  
25 SILAM forecasts, for which the satellite data were available at the specific hour.

## 3 Predicted evolution of the low-ozone area

According to the SILAM forecasts, the episode was started at the beginning of November 2018 in Atlantic Ocean south-east of Greenland by a strong storm (Figure 1a and Supplementary figures S1 – S7), which created a powerful updraught reaching up to nearly 15 km of altitude. Already then, this intrusion started affecting the stratospheric ozone concentrations  
30 over south-west of Norway but the reduction was just 10-15 DU (Figure 2a). The air masses were subsequently transported to the north-east and further lifted over the Scandinavian ridge gradually mixing with the ozone layer at 20-25km altitude



(Figure 1b, Figure 2ab). As a result, the area with anomalously thin ozone column (~200-210 DU) was formed over central and northern Finland (Figure 2b). In the following days, the eastward transport continued and the low-ozone air masses were transported towards Russia gradually dissolving over Siberia (Figure 2cd). The episode practically ended on 7.11.2018 but the ozone layer thickness remained somewhat low over Eurasia (230-240 DU) for a few days after (Figure 2d and  
5 supplementary information).

In the peak of the episode, on 4 November 2018, the ozone column over Finland was 30-35% thinner than its usual level of 300-350 DU (Figure 2).

#### 4 Evaluation of the SILAM predictions

Evaluation of the above model predictions was performed against OMI and OMPS satellite retrievals of the ozone total  
10 column, as well as against MLS vertical ozone profiles. Due to very similar patterns shown by both satellites, below we discuss the OMI-based comparison whereas the OMPS images can be found in the supplementary material. The main focus was on the model ability to reproduce the absolute level of the ozone column load, as well as on accurate location of the depletion area in space and time.

The model predictions, the shape and evolution of the low-ozone area over Scandinavia were confirmed (Figure 3 for  
15 4.11.2018 and the supplementary figures S8 - S13 for the whole period). The only issue revealed by the comparison was a pretty homogeneous under-estimation of the total ozone column by SILAM – within 10-20 DU over the bulk of the domain. This bias was also stable in time and practically did not vary throughout the episode (see supplementary material). Accounting for this correction, the actual ozone load was about 210-215 DU in the peak of the episode (whereas SILAM suggested it down to 200 DU), as compares to ~310-320 DU of a zonal-mean level between 60N and 80N (SILAM mean  
20 was about 300 DU).

The vertical distribution of the ozone loss on 4.11.2018 was predicted to span up to 25km and beyond (Figure 1b). A similar effect is also seen in the MLS retrievals (Figure 4), which show that the highest ozone concentrations during the episode were at 22-23 km instead of usual 17-18 km and were below  $7 \mu\text{mole m}^{-3}$  instead of usual  $8-10 \mu\text{mole m}^{-3}$ . One can also see that the bulk of ozone reduction occurred below the 23 km altitude level but even above that level the concentrations were in  
25 the lower quartile of the whole 60N-80N belt. This is well in agreement with the SILAM forecasts and confirms an unusually strong penetration of the tropospheric air into the stratosphere.

As mentioned in the methodological section, the SILAM global forecasts are performed without observational data assimilation, i.e. the next forecast is started from the appropriate step of the previous one. At a price of certain worsening of the formal scores, such as the model bias, this approach ensures well-balanced simulations: the quality of the forecast  
30 deteriorates only slightly over the whole predicted period (see the Supplementary material). The connection to reality is ensured by the meteorological driver IFS, which assimilates the meteorological observations at the start of each forecast.



#### 4 Discussion

Looking into the history of OMI observations, the episode was quite extreme although not the record-setting. In its depth on 4.11.2018, it corresponded to 0.5-th percentile of the ozone distribution in November north of 60N observed by OMI over the whole 12-years period of operations (2005-2017). Only three episodes, also in November (the month with the lowest ozone load in the Northern sub-polar areas), during these 12 years were stronger. Its strength was a result of coincidence of otherwise usual phenomena: storm in Northern Atlantic creating the initial WCB uplift, eastwards air mass transport over the Scandinavian ridge with additional rise, and low solar radiation in November delaying the ozone recovery. The deepest decline in the subpolar region in November was in 2009 (the observed column load was below 180 DU) followed by 2008 with minimum observed column just over 180 DU, also spanning over large area (Supplementary Figure S14). Interesting was also November of 2012 when the median level of column load was at 300 DU instead of usual 320 DU. No evident trend in median or minimum column loads in November in northern sub-polar latitudes were found over these years.

The TST intrusions are less studied in the literature compare to the STT ones, which have profound impact on the surface ozone concentrations and tropospheric ozone budget. Also, the bulk of the TST events are shallow with small impact on large-scale processes. However, Stohl (2003) pointed out that the effect of deep intrusions may be significantly larger and Reutter et al. (2015) estimated that the overall effect of these fluxes is quite comparable: just 34 % more mass is exchanged near North Atlantic cyclones for STT than for TST, average over all seasons 1979-2011.

Several other mechanisms can induce significant TST fluxes in extra-tropical regions. Powerful intrusions regularly occur along the folded tropopause in mid-latitudes. One of early modelling efforts studying this topic dates back to 1990s when the tropospheric chemistry transport model EURAD was applied to such event and reproduced its main features under a simple assumption of linear relationship between the ozone level and potential vorticity (Ebel et al., 1991). More recent diagnostic study of (Pan et al., 2009) pointed out that the association of the ozone and the thermal structure demonstrates the physical significance of the subtropical tropopause break and the secondary tropopause. However, the core of such intrusions is generally under 15km and the underlying dynamics also has little common with the current case.

The bulk impact of the episode on the large-scale atmospheric processes was small due to its intermittent limited-area character. The total reduction of the ozone amount at 12:00 4.11.2018 in comparison with the “unperturbed” level was 1.3 Tg, which is almost 30% reduction of the layer over Finland but just 0.6% of the total ozone amount in the 60N-80N belt (205 Tg, as predicted by SILAM). However, one has to keep in mind that during the stormy autumn/winter months quite a few cyclones have a capacity to create such depletion events.

From the health prospective, low UV level in November in northern latitudes also precluded any significant impact. For the future, the projected increase of the strength of storms can potentially make the tropospheric intrusions more significant players than was the current episode.

The effect of climate change on the strength and frequency of such events will probably be promotional but quantitative assessment is difficult. Indeed, as shown above, such episodes are started by strong storms. Numerous studies summarised in



IPCC Assessment Report AR5 and Special report of 1.5° global warming showed that there is a general tendency of decreasing global number of tropical cyclones and the accumulated cyclonic energy e.g., (Elsner et al., 2008), (Knutson et al., 2010), (Hoegh-Guldberg et al., 2018) and references therein. The phenomenon has been also understood from theoretical point of view (Kang and Elsner, 2015). According to these findings and future-climate projections, further decrease in cyclonic activity is likely. However, IPCC assigned low confidence to this conclusion due to a few studies reporting contradicting trends. At the same time, the number and intensity of severe cyclones and storms has increased and will probably increase further (also low confidence according to IPCC) (Knutson et al., 2013). The latter expectation is supported by e.g. statistics of strong storms in Atlantic (includes the whole of Atlantic), which shows that the number of major named storms has grown from 7 per year in 1850s to 13 in 2010s (<http://www.stormfax.com/huryear.htm>, visited 16.08.2019). The sharp growth started around 1990 adding almost 30% within last 30 years. Since the ozone mini-holes will be associated with strong storms, one can expect an increase of both frequency and strength of such events in the future.

## 5 Conclusions

An episode of a strong tropospheric intrusion into the UTLS and to the middle stratosphere was predicted by the SILAM model and subsequently observed by the ozone monitoring satellites in the first decade of November 2018.

15 The intrusion resulted in a short (~3 days) but significant (30%, , from >310 DU down to ~210 DU) regional reduction of the total ozone column. The most-significant reduction occurred over northern Scandinavia, seemingly owing to an additional enforcement of the intrusion by the lift-up over the Scandinavian ridge.

20 The episode corresponded to 0.5-th percentile of the OMI observations over the whole period 2005-2017 for the latitude belt 60N-80N in November (the month with the lowest ozone concentration in the northern sub-polar stratosphere). Despite the comparatively extreme character of the episode, its impact on the large-scale atmospheric processes and UV index at the surface was small due to intermittent character of the ozone reduction and low level of UV radiation in Northern Europe in November.

High accuracy of the episode prediction 5 days in advance by the IFS-SILAM modelling tandem illustrates the model capabilities of short-term forecasting of the stratospheric composition, including such rare events.

## 25 Data and model availability

The SILAM forecasts are openly available from <http://silam.fmi.fi> as a week-long rolling archive. Due to large size (>2 TB per day), only a subset of the forecasts is archived over the long term. That information is available on request from the authors of the paper.

SILAM is an open-code system and can be obtained from the authors of the paper upon request.



### Author's contributions

MS performed the analysis of the operational forecasts and wrote the paper; RK configured the operational forecasts, participated in the analysis and writing, RH developed the new chemistry transformation scheme and participated in writing; VS performed the satellite data analysis and participated in writing.

## 5 Acknowledgments

The SILAM stratospheric modules were developed within Finnish Academy ASTREX project (grant N 139126). The work has been performed within the GLORIA project of Academy of Finland (grant N 310373). Support of ESA SUNLIT and H2020 AirQast (grant N 776361) projects is kindly appreciated.

## References

- 10 Carslaw, K. S., Luo, B. and Peter, T.: An analytic expression for the composition of aqueous HNO<sub>3</sub>-H<sub>2</sub>SO<sub>4</sub> stratospheric aerosols including gas phase removal of HNO<sub>3</sub>, *Geophys. Res. Lett.*, 22(14), 1877–1880, 1995.
- Cunnold, D. M., Fraser, P. J., Weiss, R. F., Prinn, R. G., Simmonds, P. G., Miller, B. R., Alyea, F. N. and Crawford, A. J.: Global trends and annual releases of CCl<sub>3</sub>F and CCl<sub>2</sub>F<sub>2</sub> estimated from ALE/GAGE and other measurements from July 1978 to June 1991, *J. Geophys. Res.*, 99(D1), 1107, doi:10.1029/93JD02715, 1994.
- 15 Damski, J., Thölix, L., Backman, L., Taalas, P. and Kulmala, M.: FinROSE: middle atmospheric chemistry transport model, *Boreal Environ. Res.*, 12(5), 535–550 [online] Available from: <http://cat.inist.fr/?aModele=afficheN&cpsidt=19218894>, 2007.
- Ebel, A., Hass, H., Jakobs, H., Laube, M., Memmesheimer, M., Oberreuter, A., Geiss, H. and Kuo, Y.-H.: Simulation of ozone intrusion caused by tropopause fold and COL, *Atmos. Environ. Part A. Gen. Top.*, 25, 2131–2144, doi:10.1016/0960-20 1686(91)90089-P, 1991.
- Edwards, P. M. and Evans, M. J.: A new diagnostic for tropospheric ozone production, *Atmos. Chem. Phys.*, 17(22), 13669–13680, doi:10.5194/acp-17-13669-2017, 2017.
- Elsner, J. B., Kossin, J. P. and Jagger, T. H.: The increasing intensity of the strongest tropical cyclones, *Nat. Clim. Chang.*, 455(September), 2–5, doi:10.1038/nature07234, 2008.
- 25 Flynn, L. E., Seftor, C. J., Larsen, J. C. and Xu, P.: The Ozone Mapping and Profiler Suite, in *Earth Science Satellite Remote Sensing: Vol. 1: Science and Instruments*, edited by J. J. Qu, W. Gao, M. Kafatos, R. E. Murphy, and V. V. Salomonson, pp. 279–296, Springer Berlin Heidelberg, Berlin, Heidelberg., 2006.
- Gery, M. W., Whitten, G. Z., Killus, J. P. and Dodge, M. C.: A photochemical kinetics mechanism for urban and regional scale computer modeling, *J. Geophys. Res.*, 94(12), 12925–12956, 1989.
- 30 Granier, C., Bessagnet, B., Bond, T., D'Angiola, A., Denier van der Gon, H., Frost, G. J., Heil, A., Kaiser, J. W., Kinne, S.,



- Klimont, Z., Kloster, S., Lamarque, J.-F., Lioussé, C., Masui, T., Meleux, F., Mieville, A., Ohara, T., Raut, J.-C., Riahi, K., Schultz, M. G., Smith, S. J., Thompson, A., Aardenne, J., Werf, G. R. and Vuuren, D. P.: Evolution of anthropogenic and biomass burning emissions of air pollutants at global and regional scales during the 1980–2010 period, *Clim. Change*, 109(1–2), 163–190, doi:10.1007/s10584-011-0154-1, 2011.
- 5 Hoegh-Guldberg, O., Jacob, D., Taylor, M., Bindi, M., Brown, S., Camilloni, I., Diedhiou, A., Djalante, R., Ebi, K. L., Engelbrecht, F., Guiot, J., Hijioka, Y., Mehrotra, S., Payne, A., Seneviratne, S. I., Thomas, A., Warren, R. and Zhou, G.: Impacts of 1.5°C Global Warming on Natural and Human Systems. In: *Global Warming of 1.5°C*, in An IPCC Special Report on the impacts of global warming of 1.5°C above pre-industrial levels and related global greenhouse gas emission pathways, in the context of strengthening the global response to the threat of climate change, sustainable development, p. 10 138., 2018.
- Jaeglé, L., Wood, R. and Wargan, K.: Multiyear Composite View of Ozone Enhancements and Stratosphere-to-Troposphere Transport in Dry Intrusions of Northern Hemisphere Extratropical Cyclones, *J. Geophys. Res. Atmos.*, 122(24), 13,436–13,457, doi:10.1002/2017JD027656, 2017.
- Jalkanen, J.-P., Brink, A., Kalli, J., Pettersson, H., Kukkonen, J. and Stipa, T.: A modelling system for the exhaust emissions 15 of marine traffic and its application in the Baltic Sea area, *Atmos. Chem. Phys.*, 9(4), 9209–9223, doi:10.5194/acpd-9-15339-2009, 2009.
- Jalkanen, J. P., Johansson, L. and Kukkonen, J.: A comprehensive inventory the ship traffic exhaust emissions in the European sea areas in 2011, *Atmos. Chem. Phys.*, 16, 71–84, doi:10.5194/acp-16-71-2016, 2016.
- Kaiser, J. W., Suttie, M., Flemming, J., Morcrette, J.-J., Boucher, O., Schultz, M. G., Nakajima, T. and Yamasoe, M. A.: 20 Global Real-time Fire Emission Estimates Based on Space-borne Fire Radiative Power Observations, *AIP Conf. Proc.*, 645–648, doi:10.1063/1.3117069, 2009.
- Kang, N. and Elsner, J. B.: Trade-off between intensity and frequency of global tropical cyclones, *Nat. Clim. Chang.*, 5(July), doi:10.1038/NCLIMATE2646, 2015.
- Knutson, T. R., McBride, J. L., Chan, J., Emanuel, K., Holland, G., Landsea, C., Held, I., Kossin, J. P., Srivastava, A. K. and 25 Sugi, M.: Tropical cyclones and climate change, *Nat. Geosci.*, 3, 157 [online] Available from: <https://doi.org/10.1038/ngeo779>, 2010.
- Knutson, T. R., Sirutis, J. J., Vecchi, G. A., Garner, S., Zhao, M., Kim, H.-S., Bender, M., Tuleya, R. E., Held, I. M. and Villarini, G.: Dynamical Downscaling Projections of Twenty-First-Century Atlantic Hurricane Activity : CMIP3 and CMIP5 Model-Based Scenarios, *J. Clim.*, 26, 6591–6617, doi:10.1175/JCLI-D-12-00539.1, 2013.
- 30 Levelt, P. F., van den Oord, G. H. J., Dobver, M. R., Mälkki, A., Visser, H., de Vries, J., Stammes, P., Lundell, J. O. V and Saari, H.: The ozone monitoring instrument, *IEEE Trans. Geosci. Remote Sens.*, 44(5), 1093–1101, doi:10.1109/TGRS.2006.872333, 2006.
- Levelt, P. F., Joiner, J., Tamminen, J., Veefkind, J. P., Bhartia, P. K., Stein Zweers, D. C., Duncan, B. N., Streets, D. G., Eskes, H., van der A, R., McLinden, C., Fioletov, V., Carn, S., de Laat, J., DeLand, M., Marchenko, S., McPeters, R.,

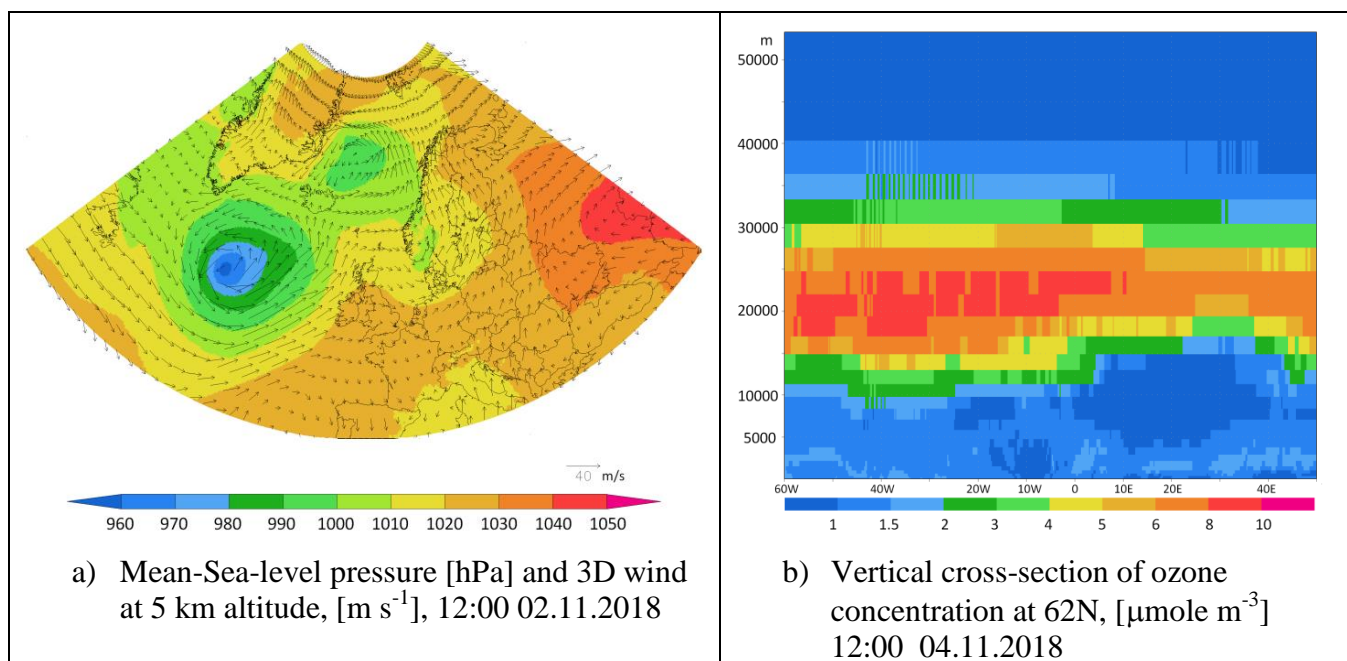




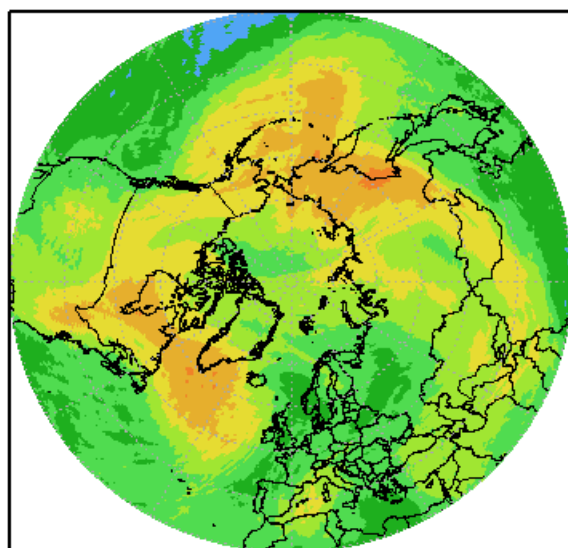
- Ziemke, J., Fu, D., Liu, X., Pickering, K., Apituley, A., González Abad, G., Arola, A., Boersma, F., Chan Miller, C., Chance, K., de Graaf, M., Hakkarainen, J., Hassinen, S., Ialongo, I., Kleipool, Q., Krotkov, N., Li, C., Lamsal, L., Newman, P., Nowlan, C., Suleiman, R., Tilstra, L. G., Torres, O., Wang, H. and Wargan, K.: The Ozone Monitoring Instrument: overview of 14 years in space, *Atmos. Chem. Phys.*, 18(8), 5699–5745, doi:10.5194/acp-18-5699-2018, 2018.
- 5 Lobert, J. M., Keene, W. C., Logan, J. A. and Yevich, R.: Global chlorine emissions from biomass burning: Reactive Chlorine Emissions Inventory, *J. Geophys. Res.*, 104(D7), 8373–8389, 1999.
- Olsen, M. A., Douglass, A. R. and Kaplan, T. B.: Variability of extratropical ozone stratosphere–troposphere exchange using microwave limb sounder observations, *J. Geophys. Res. Atmos.*, 118(2), 1090–1099, doi:10.1029/2012JD018465, 2013.
- Orbe, C., Waugh, D. W. and Newman, P. A.: Air-mass origin in the tropical lower stratosphere: The influence of Asian boundary layer air, *Geophys. Res. Lett.*, 42(10), 4240–4248, doi:10.1002/2015GL063937, 2015.
- 10 Pan, L. L., Randel, W. J., Gille, J. C., Hall, W. D., Nardi, B., Massie, S., Yudin, V., Khosravi, R., Konopka, P. and Tarasick, D.: Tropospheric intrusions associated with the secondary tropopause, *J. Geophys. Res.*, 114(D10302), 1–12, doi:10.1029/2008JD011374, 2009.
- Price, C., Penner, J. and Prather, M.: NO<sub>x</sub> from lightning: 1. Global distribution based on lightning physics, *J. Geophys. Res.*, 102, 5929, doi:10.1029/96JD03504, 1997.
- 15 Reutter, P., Škerlak, B., Sprenger, M. and Wernli, H.: Stratosphere-troposphere exchange (STE) in the vicinity of North Atlantic cyclones, *Atmos. Chem. Phys.*, 15(19), 10939–10953, doi:10.5194/acp-15-10939-2015, 2015.
- Roelofs, G. and Lelieveld, J.: Tropospheric ozone simulation with a chemistry-general circulation model: Influence of higher hydrocarbon chemistry, *J. Geophys. Res.*, 105(D18), 22,697–22,712, 2000.
- 20 Sindelarova, K., Granier, C., Bouarar, I., Guenther, A., Tilmes, S., Stavrou, T., Müller, J. F., Kuhn, U., Stefani, P. and Knorr, W.: Global data set of biogenic VOC emissions calculated by the MEGAN model over the last 30 years, *Atmos. Chem. Phys.*, 14(17), 9317–9341, doi:10.5194/acp-14-9317-2014, 2014.
- Sofiev, M.: A model for the evaluation of long-term airborne pollution transport at regional and continental scales, *Atmos. Environ.*, 34(15), 2481–2493, 2000.
- 25 Sofiev, M., Vankevich, R., Lotjonen, M., Prank, M., Petukhov, V., Ermakova, T., Koskinen, J. and Kukkonen, J.: An operational system for the assimilation of the satellite information on wild-land fires for the needs of air quality modelling and forecasting, *Atmos. Chem. Phys.*, 9(18), 2009.
- Sofiev, M., Soares, J., Prank, M., Leeuw, G. and Kukkonen, J.: A regional-to-global model of emission and transport of sea salt particles in the atmosphere, *J. Geophys. Res.*, 116(D21302), 25, doi:10.1029/2010JD014713, 2011.
- 30 Sofiev, M., Vankevich, R., Ermakova, T. and Hakkarainen, J.: Global mapping of maximum emission heights and resulting vertical profiles of wildfire emissions, *Atmos. Chem. Phys.*, 13(14), 7039–7052, doi:10.5194/acp-13-7039-2013, 2013.
- Sofiev, M., Vira, J., Kouznetsov, R., Prank, M., Soares, J. and Genikhovich, E.: Construction of the SILAM Eulerian atmospheric dispersion model based on the advection algorithm of Michael Galperin, *Geosci. Model Dev.*, 8(11), 3497–3522, doi:10.5194/gmd-8-3497-2015, 2015.



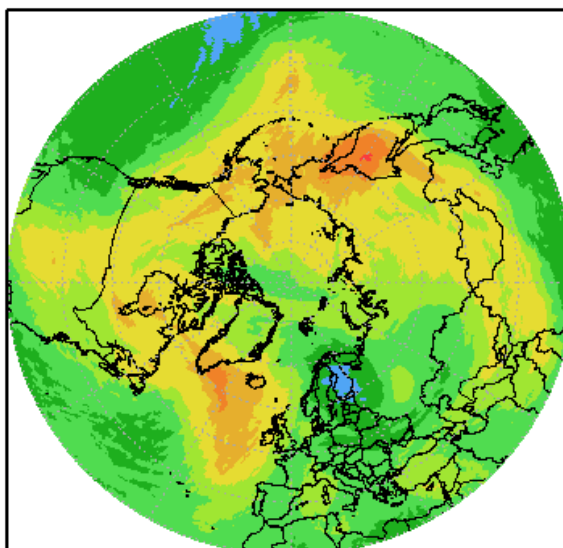
- Sofiev, M., Winebrake, J. J., Johansson, L., Carr, E. W., Prank, M., Soares, J., Vira, J., Kouznetsov, R., Jalkanen, J.-P. and Corbett, J. J.: Cleaner fuels for ships provide public health benefits with climate tradeoffs, *Nat. Commun.*, 9(1), 406, doi:10.1038/s41467-017-02774-9, 2018.
- Stohl, A.: A 1-year Lagrangian “climatology” of airstreams in the Northern Hemisphere troposphere and lowermost stratosphere, *J. Geophys. Res. Atmos.*, 106(D7), 7263–7279, doi:10.1029/2000JD900570, 2001.
- 5 Stohl, A.: Stratosphere-troposphere exchange: A review, and what we have learned from STACCATO, *J. Geophys. Res.*, 108(D12), doi:10.1029/2002jd002490, 2003.
- Waters, J. W., Froidevaux, L., Harwood, R. S., Jarnot, R. F., Pickett, H. M., Read, W. G., Siegel, P. H., Cofield, R. E., Filipiak, M. J., Flower, D. A., Holden, J. R., Lau, G. K. K., Livesey, N. J., Manney, G. L., Pumphrey, H. C., Santee, M. L.,  
10 Wu, D. L., Cuddy, D. T., Lay, R. R., Loo, M. S., Perun, V. S., Schwartz, M. J., Stek, P. C., Thurstans, R. P., Boyles, M. A., Chandra, K. M., Chavez, M. C., Chen, G. S., Chudasama, B. V., Dodge, R., Fuller, R. A., Girard, M. A., Jiang, J. H., Jiang, Y. B., Knosp, B. W., LaBelle, R. C., Lam, J. C., Lee, K. A., Miller, D., Oswald, J. E., Patel, N. C., Pukala, D. M., Quintero, O., Scaff, D. M., Van Snyder, W., Tope, M. C., Wagner, P. A. and Walch, M. J.: The Earth Observing System Microwave Limb Sounder (EOS MLS) on the Aura satellite, *IEEE Trans. Geosci. Remote Sens.*, 44(5), 1075–1092,  
15 doi:10.1109/TGRS.2006.873771, 2006.



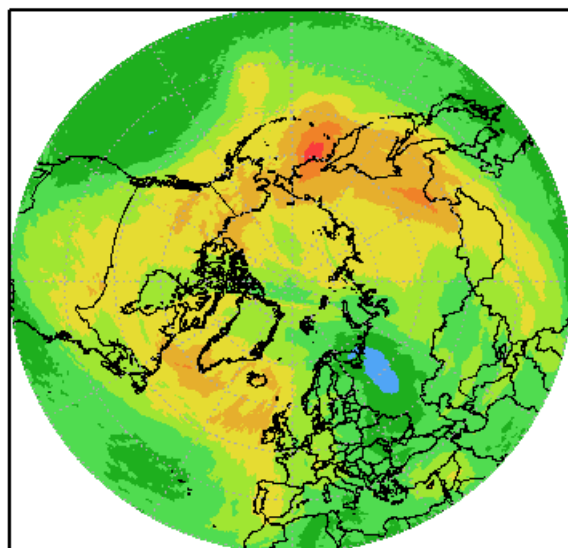
5 **Figure 1. Meteorological situation at 12:00 3.11.2018 (panel a, shades showing the sea-level pressure, hPa and vectors presenting wind at 8-th SILAM hybrid model level, ~1830 m above the ground) and vertical ozone profiles at latitude 62N at 12:00 4.11.2018. (right panel, ozone concentration  $\mu\text{mole m}^{-3}$ )**



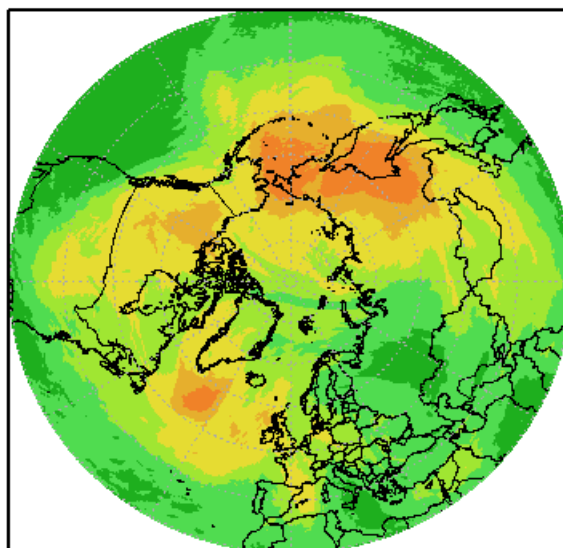
a) 12:00 03.11.2018, +59 hrs forecast



b) 12:00 04.11.2018, +83 hrs forecast



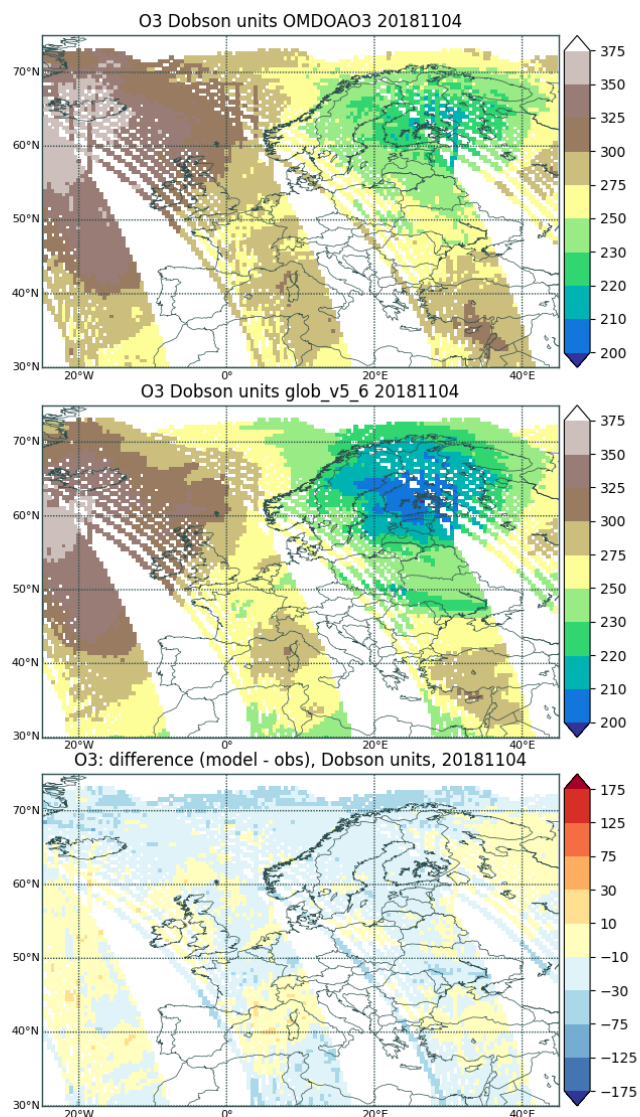
c) 12:00 05.11.2018, +107 hrs forecast



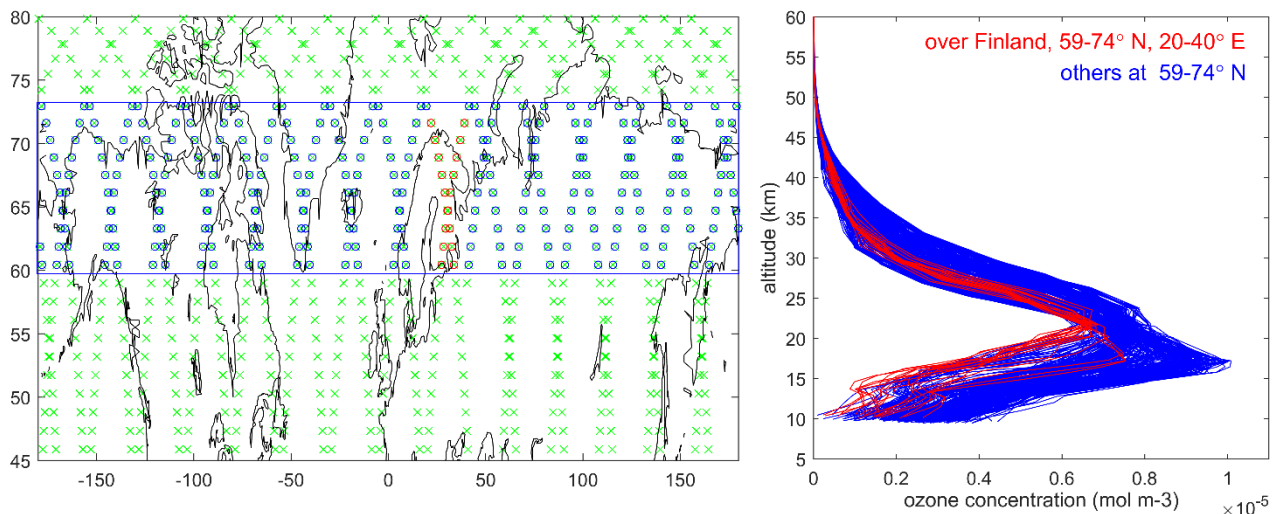
d) 12:00 06.11.2018, +131 hrs forecast



Figure 2. Mid-day (UTC time) total ozone column in DU (Dobson units) for 3.11 – 6.11.2018 as predicted by SILAM model on 1.11.2018. Forecast length were from +59 for panel a till- +131 hours for panel d



5 **Figure 3. Daily-composite ozone column (DU) for 4.11.2018 observed by OMI DOAS (upper panel) and predicted by SILAM (middle panel). Only grid cells corresponding to valid OMI observations were retained in the SILAM forecast. Bottom panel: difference modelled minus observed ozone column (DU).**



**Figure 4.** Left: locations of the MLS ozone profiles on 4.11.2018, latitude belt 59N-74N and longitudinal range 20E-40E are highlighted by blue and red d, respectively. Right: MLS ozone vertical profiles in the highlighted regions: over Finland, lon-lat box 59N-74N × 20E – 40E (red) and other profiles at latitudes 59N-74N (blue).

5